Biophysical Chemistry 6 (1977) 107–115
© North-Holland Publishing Company

THREE STEADY STATE SITUATION IN AN OPEN CHEMICAL REACTION SYSTEM. I

W. GEISELER and H.H. FÖLLNER

Institut für Physikalische Chemie der Rheinisch Westfälischen Technischen Hochschule Aachen, D-51 Aachen, Germany

Received 20 June 1976
Revised manuscript received 10 September 1976

In an isothermal continuously stirred tank reactor (open chemical reaction system) fed by sulphuric acid solutions of bromate, bromide and cerium(III) bistability (three steady state situation) is experimentally observed. This remarkable behavior, based on the instability of one steady state, has important consequences for the understanding of excitability and biochemical control mechanisms. The mass-balance equations for the reactor and the chemical mechanism of the reaction are combined into a simple mathematical model. The behavior of the resulting nonlinear differential equations is examined analytically and by a graphical integration procedure (method of isoclines). Using realistic kinetic data, the model shows the same behavior as observed in the experiment.

1. Introduction

Multi-steady state situations in homogeneous chemical reactions have been predicted to exist in open systems under conditions far from equilibrium [1]. This remarkable behavior has been shown to be caused by the nonlinear kinetics that may arise through feedback mechanisms (e.g., autocatalysis) [2, 3, 4]. As shown in fig. 1 the three steady state situation for a system described by two independent variables can be illustrated conveniently in the phase plane [5]. The system considered here can exist in two stable steady

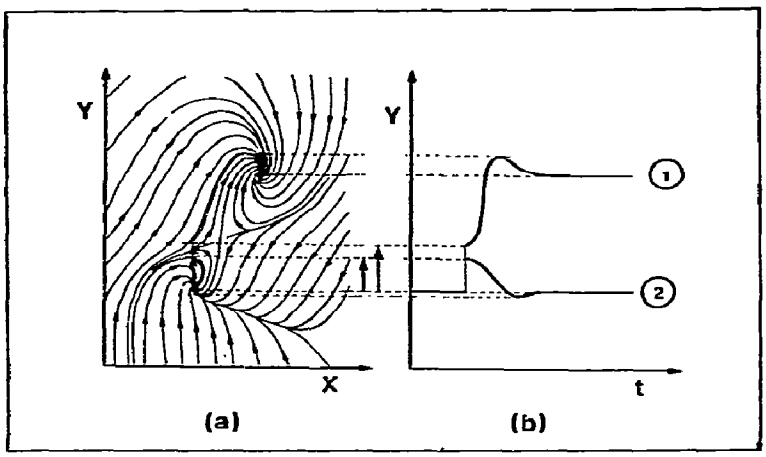

Fig. 1. Three steady state situation [two stable states (foci) and one unstable state (saddle point)] in the phase plane of an arbitrary system which is described by two independent variables (a). The lines represent non-stationary states (trajectories) along which the system evolves to the steady states. The temporal response of the system to both super-threshold (1) and sub-threshold (2) stimuli (big and small arrows) is derived from the phase plane (b). Curves of this type are frequently observed in excitable biological systems (from [6]).

states (foci). The third steady state (saddle point) is unstable and gives rise to excitability phenomena extensively described in [2]. The evolution of the system to a new stable steady state as the result of a super-threshold stimulus (big arrow) is shown on the right-hand side of fig. 1. A sub-threshold stimulus (small arrow) does not give rise to a transition but acts as a perturbation on the steady state of the system.

The first report on bistability (three steady state situation) in a real chemical reaction system (peroxidase catalysed oxidation of NADH by O_2) appeared in 1968 [7]. Since then a few autocatalytic reactions combined with an inhibitional reaction step have been found to exhibit bistability when carried out in a continuously stirred tank reactor (CSTR) [8,9]. No mathematical model, using kinetic data obtained from experiment, has been proposed for those systems. Recently bistable behavior arising in homogeneous chemical reaction systems has attracted new interest and has especially been discussed for the oscillating Belousov–Zhabotinskii reaction (BZR) [10].

In the present paper we shall report in detail the autocatalytic bromate–bromide–cerium(III) reaction taking place in the CSTR. The behavior of this reaction system has been described qualitatively in [9]. The mathematical model we shall propose is based on experimental data and on kinetic data presented in [11, 12]. Finally we shall examine the resulting system of nonlinear differential equations analytically and integrate them by application of a graphical integration procedure (method of isoclines [5]).

2. Reaction system

The reaction system we consider is the ideal CSTR containing a sulphuric acid solution of bromate, bromide and cerium(III). The reactor consists of a well-stirred tank with a steady inflow of reactive materials (bromate, bromide and cerium (III) in sulphuric acid solution) and a continuous outflow of (partially) reacted materials [9]. The chemical reaction taking place in the reactor is the autocatalytic oxidation of cerium(III) by bromate in the presence of bromide and represents the pure inorganic subsystem of the BZR. This nonoscillatory subsystem includes the trigger process which in combination with a suitable regeneration step (organic compounds) gives rise to oscillatory behavior. The overall reaction may be written as:

$$2HBrO_3 + 2HBr + 2Ce_2(SO_4)_3 + 2H_2SO_4 \rightarrow 4Ce(SO_4)_2 + 4HOBr + 2H_2O . \quad (1)$$

We derive the chemical mechanism from the detailed kinetics of the oscillating Belousov–Zhabotinskii reaction published by Field, Körös and Noyes (FKN) [12,13]. Omitting the organic species and applying bromide the mechanism of the overall process (1) can be described by the following chemical processes:

$$BrO_3^- + Br^- + 2H^+ \xrightarrow{k_{R3}} HBrO_2 + HOBr , \quad (2)$$

$$Br^- + HBrO_2 + H^+ \xrightarrow{k_{R2}} 2HOBr , \quad (3)$$

$$BrO_3^- + HBrO_2 + H^+ \xrightarrow{k_{R5}} [2BrO_2^- + H_2O , \quad (4)$$

$$BrO_2^- + Ce^{3+} + H^+ \rightarrow [\ Ce^{4+} + HBrO_2 , \quad (5)$$

$$2HBrO_2 \xrightarrow{k_{R4}} BrO_3^- + HOBr + H^+ . \quad (6)$$

The rate constant subscripts refer to the constants chosen by FKN [13]. The complete chemical mechanism is considerably more complicated, but the simplified version presented here is sufficient for the description of the bistable behavior of the system.

In accordance to FKN steps (2), (3) and (5) are assumed to be bimolecular elementary processes. Furthermore, step (4) is rate-determining for the overall autocatalytic process [(4) + 2(5)] to which bromide is a strong inhibitor [14]. Cerium(IV) ions produced in step (5) are not assumed to be reduced by any chemical reaction.

3. Experimental section

A stirred glass tank reactor which could be operated both batchwise and continuously was employed [9]. The temperature of the reaction mixture was kept constant (25°C) by means of a water flow through the cooling jacket of the tank. The volume V_R occupied by the reaction mixture was 0.1 ℓ. During the reaction the concentrations of bromide and cerium(IV) were recorded continuously by potentiometric and spectrophotometric techniques. In the first case an electrode specifically sensitive to bromide was used. In the second

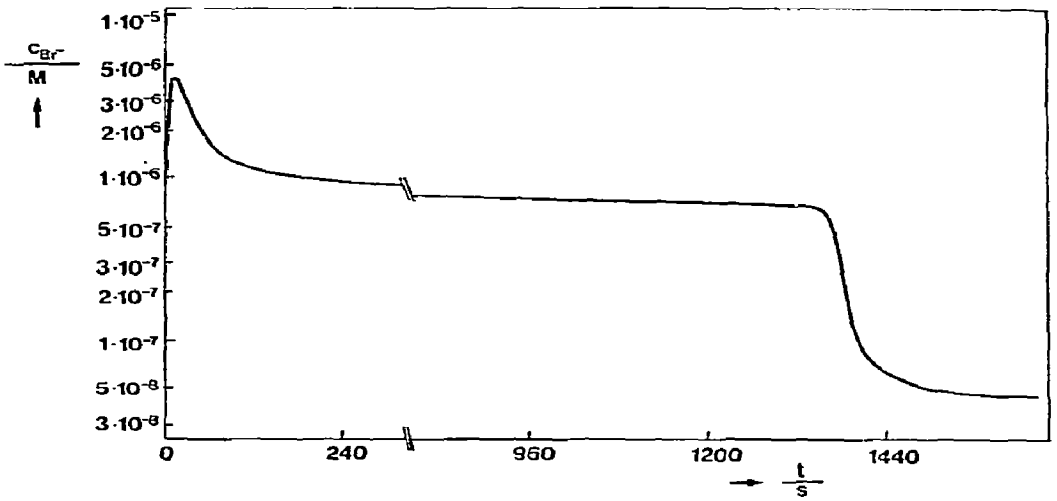

Fig. 2. Typical plot of the autocatalytic reaction containing initially bromate, bromide and cerium(III) in sulphuric acid solution (reactor operating batchwise). Initial concentrations were: $[KBrO_3]_0 = 2 \times 10^{-3}$ M, $[KBr]_0 = 10^{-5}$ M, $[(NH_4)_2Ce(NO_3)_5 \cdot 6H_2O]_0 = 1.5 \times 10^{-4}$ M. Solvent: $[H_2SO_4] = 1.5$ M. $T = 25°C$. Reactor volume $V_R = 10^{-1}$ ℓ.

case blue light ($\lambda = 402$ nm) was employed. The intensity was measured by means of a photomultiplier.

In fig. 2 a representative result is shown for an experiment carried out in the batchwise operating reactor. Initially containing a sulphuric acid solution of bromate the reactor was started up by rapidly adding a mixture of cerium(III) and bromide in sulphuric acid solution. The initial concentrations of the reacting substances are indicated in the legend of the figure. From the potentiometric trace of the bromide sensitive electrode it can be seen that a fast bromide consumption period occurs initially. It is followed by a quasisteady state period wherein the consumption of bromide is very slow. At a certain time a critical value of the concentration of bromide is achieved and the inhibitional effect of bromide to the autocatalytic reaction step ceases. The rate of the autocatalysis accelerates and gives rise to further depletion of bromide. Finally a low quasi-steady state concentration is attained.

Fig. 3 illustrates the typical bistable behavior of the reaction when carried out in the isothermal CSTR [9]. The upper curve records the potential of the bromide sensitive electrode. The lower curve records the concentration of cerium(III) obtained spectrophotometrically. It has been derived from the spectrophotometric signal of the cerium(IV) ions which are assumed to be the only other cerium species. The experiment was started up as a batch experiment but was immediately continued by entering of three separate feed streams namely sulphuric acid solutions of bromate, bromide and cerium(III). The concentrations of the feed materials in the inlet streams were chosen in such a way, that the resulting inlet concentrations directly after mixing were equal to the initial concentrations used in the batchwise operating reactor.

From fig. 3 we recognize that the system can operate in two different stable steady states corresponding to different steady state concentrations of bromide and cerium(III). The transition from one stable steady state to the other is a trigger process obeying the all-or-nothing law of excitation. There also exists one unstable steady state situated between the two stable states. It is characterised by a critical concentration of bromide ($\sim 10^{-6}$ M). With respect to stimuli the unstable steady state plays the role of critical state dividing the kinetic behavior of the system into two ranges. The transition from one stable steady state to the other requires super-threshold stimuli. Being in the upper (lower) stable steady state the system can be stimulated by decreasing (increasing) the inlet flow concentration of bromide for a short time. The effects of both super- and sub-threshold stimuli are also shown in fig. 3. The small arrows indicate the moments the

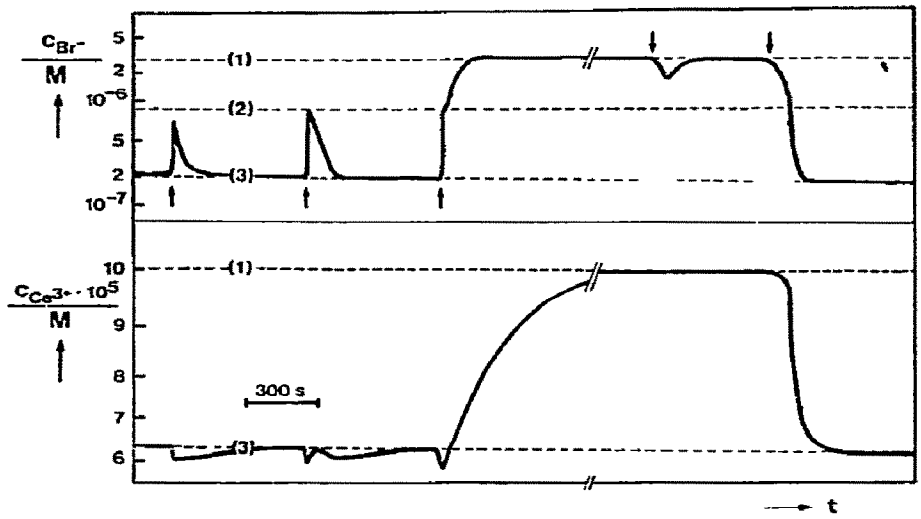

Fig. 3. Typical plot of the bistable behavior of the autocatalytic reaction carried out in an isothermal CSTR. Initial and inlet concentrations: $[KBrO_3]_0 = 2 \times 10^{-3}$ M, $[KBr]_0 = 10^{-5}$ M, $[(NH_4)_2Ce(NO_3)_5 \cdot 6H_2O]_0 = 1.5 \times 10^{-4}$ M. Solvent: $[H_2SO_4] = 1.5$ M. $T = 25°C$. Reactor volume $V_R = 10^{-1}$ ℓ. Total flow rate $\dot{V} = 4 \times 10^{-4}$ ℓs^{-1} (from [9]).

stimuli were applied. Details on strength and duration of the applied stimuli may be found in [9,23].

The long-lasting rise of cerium(III) reflects the material flow and is not affected by any chemical reaction. During this period the autocatalytic reaction step is completely inhibited by bromide.

4. Mathematical model

4.1. Constitution of the model system

In this section a mathematical model for the bistable reaction system is developed. For the chemical mechanism presented by eqs. (2)–(6) the chemical species BrO_3^-, Ce^{3+}, Br^- supplied to the reactor and the intermediate $HBrO_2$ are assumed to be the essential variables. By application of the mass-balance equation we obtain the following system of nonlinear differential equations:

$$\dot{A} = k_0 A_0 - k_{R3} H_0^2 A Y - k_{R5} A H_0 X + k_{R4} X^2 - k_0 A , \tag{7}$$

$$\dot{X} = k_{R3} A H_0^2 Y - k_{R2} H_0 X Y + k_{R5} A H_0 X - 2k_{R4} X^2 - k_0 X , \tag{8}$$

$$\dot{Y} = k_0 Y_0 - k_{R3} H_0^2 A Y - k_{R2} H_0 X Y - k_0 Y , \tag{9}$$

$$\dot{Z} = k_0 Z_0 - k_{R5} A H_0 X - k_0 Z . \tag{10}$$

The following abbreviations are used here for the concentrations of the chemical species* (see [13]): $A \equiv [BrO_3^-]$, $X \equiv [HBrO_2]$, $Y \equiv [Br^-]$, $Z \equiv [Ce^{3+}]$, $H \equiv [H^+]$. The rate constant k_0 results from the constant inlet and outlet flow of the feed materials and the reaction mixture respectively. It is calculated from $k_0 = \dot{V}/V_R$ ($\dot{V}$: total flow rate through the tank; V_R: volume of the tank). In the above equations the subscript zero is also used to indicate the feed materials. Furthermore, it can be seen from the equation system that the tank is fed by all essential chemical individuals but X. This species is not assumed to be present in any feed solution.

As shown elsewhere [14] bromate and cerium(III) are not consumed completely during the overall reaction (1). From this fact and because of the excess concentration of bromate used in the experiments we estimate the variation of bromate to be only about 5%. Therefore we regard the concentration of bromate to remain constant ($\dot{A} = 0$; $A = A_0 = \text{const.}$). Thus we obtain:

* In contrast to FKN [13] the symbol Z designates the concentration of Ce^{3+} instead of Ce^{4+}.

Table 1
Rate constants and concentrations of the feed materials

Rate constant	Ref.	Feed concentration
$k_{R2} = 2 \times 10^9 M^{-2} s^{-1}$	[12,13]	$A_0 = 2 \times 10^{-3} M$
$k_{R3} = 2.1 M^{-3} s^{-1}$	[12,13]	$H_0 = 1.5 M$
$k_{R4} = 4 \times 10^7 M^{-1} s^{-1}$	[12,13]	$X_0 = 0 M$
$k_{R5} = 10^4 M^{-2} s^{-1}$	[12,13]	$Y_0 = 10^{-5} M$
$k_0 = 4.5 \times 10^{-3} s^{-1}$	this work	$Z_0 = 1.5 \times 10^{-4} M$

$$\dot{X} = k_{R3} A_0 H_0^2 Y - k_{R2} H_0 XY + k_{R5} A_0 H_0 X - 2k_{R4} X^2 - k_0 X , \quad (11)$$

$$\dot{Y} = k_0 Y_0 - k_{R3} H_0^2 A_0 Y - k_{R2} H_0 XY - k_0 Y , \quad (12)$$

$$\dot{Z} = k_0 Z_0 - k_{R5} A_0 H_0 X - k_0 Z . \quad (13)$$

Eqs. (11)–(13) can be handled more easily by introducing the new abbreviations $\alpha_1, ..., \alpha_7$:

$$\dot{X} = \alpha_1 Y - \alpha_2 XY + (\alpha_3 - \alpha_5) X - \alpha_4 X^2 = F(X, Y), \quad (14)$$

$$\dot{Y} = \alpha_6 - (\alpha_1 + \alpha_5) Y - \alpha_2 XY = G(X, Y) , \quad (15)$$

$$\dot{Z} = \alpha_7 - \alpha_5 Z - \alpha_3 X , \quad (16)$$

where

$$\alpha_1 = k_{R3} A_0 H_0^2 = 9.5 \times 10^{-3} s^{-1} ,$$

$$\alpha_2 = k_{R2} H_0 = 3 \times 10^9 M^{-1} s^{-1} ,$$

$$\alpha_3 = k_{R5} A_0 H_0 = 30 s^{-1} ,$$

$$\alpha_4 = 2k_{R4} = 8 \times 10^7 M^{-1} s^{-1} ,$$

$$\alpha_5 = k_0 = 4.5 \times 10^{-3} s^{-1} ,$$

$$\alpha_6 = k_0 Y_0 = 4.5 \times 10^{-8} M s^{-1} ,$$

$$\alpha_7 = k_0 Z_0 = 6.7 \times 10^{-7} M s^{-1} .$$

The rate constants and the concentrations of the feed solutions are listed in table 1.

Eqs. (14) and (15) do not depend on the variable Z. Making use of the solution $X(t)$ obtained from eqs. (14) and (15) eq. (16) can be solved immediately by means of the convolution integral:

$$Z(t) = Z(0) - \alpha_3 \int_0^t \exp[-\alpha_5 (t - t')] X(t') \, dt' , \quad (17)$$

where

$$Z(0) = \alpha_7 / \alpha_5 .$$

By now the equation system (7)–(10) is reduced to two nonlinear differential equations. For studying such systems some general mathematical methods have been developed [5,15]. Because of the wide range occupied both by the rate constants and by the concentrations of the chemical individuals the numerical integration procedure requires special integration techniques [13,16–20]. Therefore a topological investigation in the X-Y phase plane and a graphical integration procedure (method of isoclines) were employed.

The graphical method for integrating the differential equation system (14) and (15) starts with the calculation of the isoclines I. Dividing eq. (15) by eq. (14) yields the differential equation:

$$\frac{dY}{dX} = \frac{\alpha_6 - (\alpha_1 + \alpha_5) Y - \alpha_2 XY}{\alpha_1 Y - \alpha_2 XY + (\alpha_3 - \alpha_5) X - \alpha_4 X^2} . \quad (18)$$

For fixed values $m = dY/dX$ this equation describes the isoclines I_m which intersect the trajectories $R(t) = (X(t), Y(t))$ – the solution of equations (14) and (15) for various initial conditions – in points with slope m. By constructing a sufficient number of isoclines we can draw the solution curves belonging to different initial conditions (fig. 4).

We are able to regain the time scale by means of the equation:

$$t = \int_{Y(0)}^{Y} \frac{dY}{G(X(Y), Y)} \quad (19)$$

In fig. 4 the temporal evolution of the system to the stable steady states is also illustrated.

4.2. Determination of the steady states

The intersections of the isoclines I (singular points) represent the steady states to which the system evolves for $|t| \to \infty$. The steady states can be calculated easily by means of the isoclines I_0 (slope 0) and I_∞ (slope ∞):

$$I_0 : \quad Y = \alpha_6 / [\alpha_2 X + (\alpha_1 + \alpha_5)] , \quad (20)$$

$$I_\infty : \quad Y = [\alpha_4 X^2 - (\alpha_3 - \alpha_5) X] / (\alpha_1 - \alpha_2 X) . \quad (21)$$

The general shape of these isoclines (called nullclines) is shown in fig. 5.

From both eqs. (20) and (21) we obtain the cubic equation:

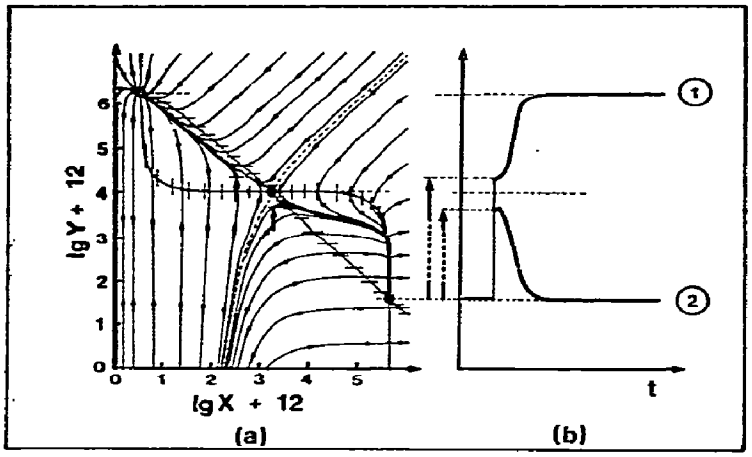

Fig. 4. Plot of the trajectories of the model system in the X-Y phase plane (a). The temporal response of the system to both super-threshold (1) and sub-threshold (2) stimuli (big and small arrows) is derived from the phase plane (b).

$$X^3 - \frac{\alpha_2(\alpha_3-\alpha_5)-\alpha_4(\alpha_1+\alpha_5)}{\alpha_2\alpha_4}X^2 + \frac{\alpha_2\alpha_6-(\alpha_3-\alpha_5)(\alpha_1+\alpha_5)}{\alpha_2\alpha_4}X - \frac{\alpha_6\alpha_1}{\alpha_2\alpha_4} = 0 \qquad (22)$$

From the sequence of the signs of the coefficients (+ − + −) we conclude that three steady states may exist in the physically relevant positive quadrant of the X-Y phase plane provided that the parameters α_5, α_6 are suitable chosen (note that the other parameters of the system are fixed by the chemical mechanism). Numerical calculation gives the values listed in table 2.

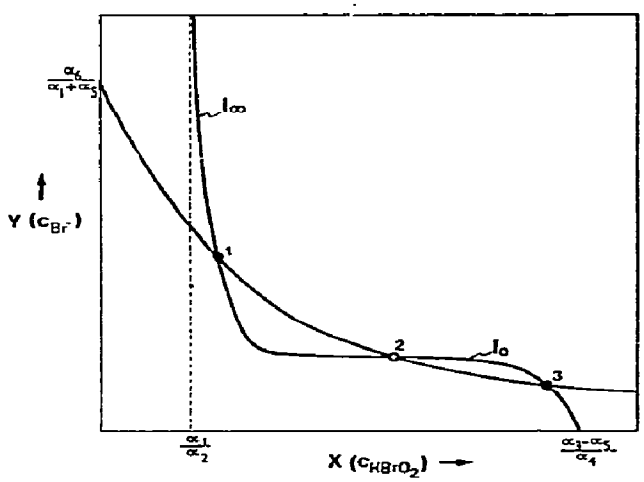

Fig. 5. The qualitative shape of the nullclines in the X-Y phase plane.

4.3. Analysis of stability of the steady states

For analysing the behavior of the trajectories in the neighbourhood of the steady states is is sufficient (under appropriate conditions) to investigate the linearised system obtained by Taylor series expansion of $F(X, Y)$ and $G(X, Y)$. Let ξ and η be deviations from the steady state under consideration:

$$\xi = X - X_{ss}, \qquad \eta = Y - Y_{ss}.$$

Then we get:

$$\dot{\xi} = \left.\frac{\partial F}{\partial X}\right|_{ss}\xi + \left.\frac{\partial F}{\partial Y}\right|_{ss}\eta, \qquad (23)$$

$$\dot{\eta} = \left.\frac{\partial G}{\partial X}\right|_{ss}\xi + \left.\frac{\partial G}{\partial Y}\right|_{ss}\eta. \qquad (24)$$

By introducing

Table 2
Steady states and eigenvalues (computed from the model)

$X_{ss}^{(1)} = 3.2\times10^{-12}$ M	$X_{ss}^{(2)} = 1.5\times10^{-9}$ M	$X_{ss}^{(3)} = 3.7\times10^{-7}$ M
$Y_{ss}^{(1)} = 1.9\times10^{-6}$ M	$X_{ss}^{(2)} = 1\times10^{-8}$ M	$Y_{ss}^{(3)} = 4\times10^{-11}$ M
$\lambda_{ss}^{(1)} = -2.3\times10^{-2}\,s^{-1}$	$\lambda_{ss}^{(2)} = 9.4\,s^{-1}$	$\lambda_{ss}^{(3)} = -3\times10^{1}\,s^{-1}$
$\lambda_{ss}^{(1)} = -5.7\times10^{3}\,s^{-1}$	$\lambda_{ss}^{(2)} = -14\,s^{-1}$	$\lambda_{ss}^{(3)} = -1.1\times10^{3}\,s^{-1}$

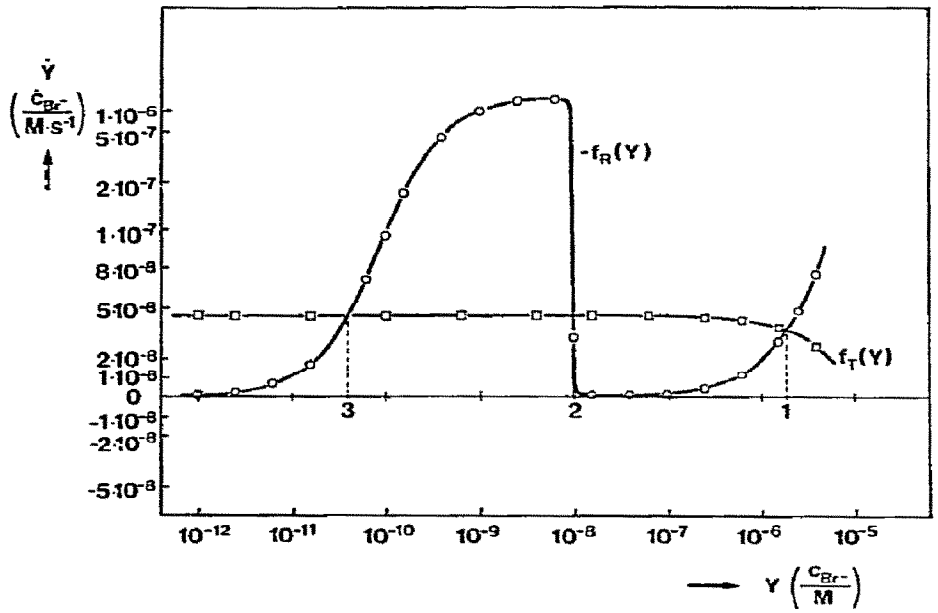

Fig. 6. The plot of the functions $f_T(Y)$ and $-f_R(Y)$ derived from eq. (28).

$$\left.\frac{\partial F}{\partial X}\right|_{ss} = A_{11}, \quad \left.\frac{\partial F}{\partial Y}\right|_{ss} = A_{12},$$

$$\left.\frac{\partial G}{\partial X}\right|_{ss} = A_{21}, \quad \left.\frac{\partial G}{\partial Y}\right|_{ss} = A_{22},$$

we obtain:

$$\begin{pmatrix}\dot{\xi}\\ \dot{\eta}\end{pmatrix} = \begin{pmatrix}A_{11} & A_{12}\\ A_{21} & A_{22}\end{pmatrix}\begin{pmatrix}\xi\\ \eta\end{pmatrix}. \tag{25}$$

The matrix A_{ik} is given by

$$A_{11} = -\alpha_2 Y_{ss} - 2\alpha_4 X_{ss} + (\alpha_3 - \alpha_5),$$

$$A_{12} = \alpha_1 - \alpha_2 X_{ss},$$

$$A_{21} = -\alpha_2 Y_{ss},$$

$$A_{22} = -(\alpha_1 + \alpha_5) - \alpha_2 X_{ss}.$$

The characteristic equation (26) gives information about the nature of the steady states:

$$\lambda^2 - (A_{11} + A_{22})\lambda + (A_{11}A_{22} - A_{21}A_{12}) = 0, \tag{26}$$

or

$$\lambda_{1,2} = \tfrac{1}{2}(A_{11} + A_{22}) \pm \tfrac{1}{2}\sqrt{(A_{11} + A_{22})^2 - 4(A_{11}A_{22} - A_{12}A_{21})}.$$

Thus we obtain for the three steady states (see also table 2):

$X_{ss}^{(1)}, Y_{ss}^{(1)}$: stable node

($\lambda_{1,2} < 0$, real valued),

$X_{ss}^{(2)}, Y_{ss}^{(2)}$: saddle point

($\lambda_1 < 0, \lambda_2 > 0$, real valued),

$X_{ss}^{(3)}, Y_{ss}^{(3)}$: stable node

($\lambda_{1,2} < 0$, real valued).

4.4. Dynamical diagram

Bistable behavior can be described using only one first order differential equation [2,21]. As shown in [13] the special character of the variable X motivates the application of quasistationarity to this species. $\dot{X} = 0$ leads to:

$$X = \frac{\alpha_3 - \alpha_5 - \alpha_2 Y}{2\alpha_4} + \sqrt{\frac{(\alpha_3 - \alpha_5 - \alpha_2 Y)^2}{4\alpha_4^2} + \frac{\alpha_1}{\alpha_4} Y}. \tag{27}$$

Replacing X of eq. (15) by eq. (27) yields:

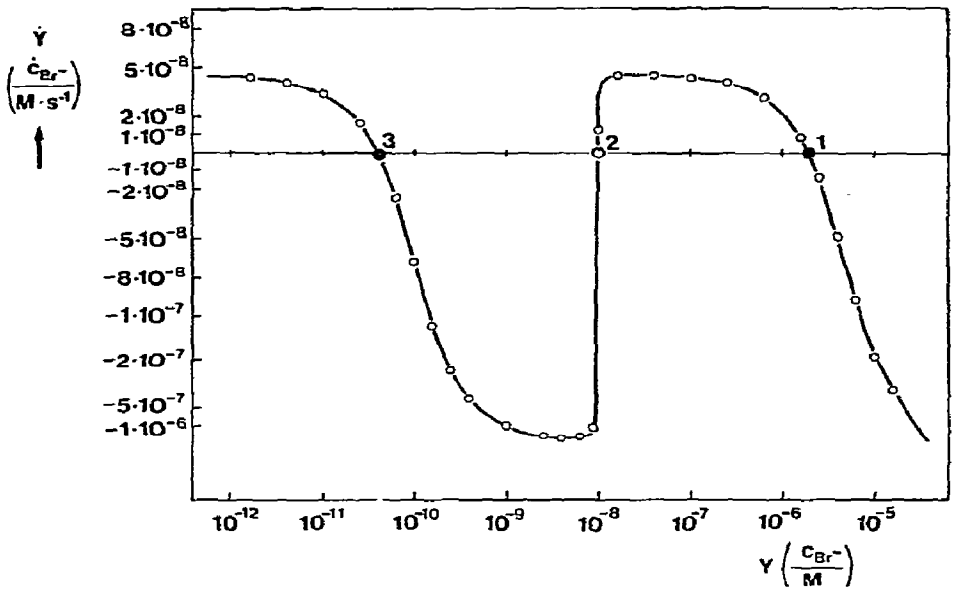

Fig. 7. Dynamical diagram.

$$\dot{Y} = \alpha_6 - \alpha_5 Y - \left(\alpha_1 + \frac{\alpha_2}{2\alpha_4}(\alpha_3 - \alpha_5)\right) Y + \frac{\alpha_2^2}{2\alpha_4} Y^2$$

$$- \frac{\alpha_2}{2\alpha_4} Y\sqrt{\alpha_2^2 Y^2 + [4\alpha_1\alpha_4 - 2\alpha_2(\alpha_3 - \alpha_5)]Y + (\alpha_3 - \alpha_5)^2} \qquad (28)$$

$$= f(Y) .$$

Thus the differential equation system (11, 12) is reduced to $\dot{Y} = f(Y)$. This function can be split into two terms, $f_T(Y)$ describing the material flow through the tank, and $f_R(Y)$ describing the rates of the chemical reactions. Thus we obtain:

$$f(Y) = f_R(Y) + f_T(Y) , \qquad (29)$$

where

$$f_T(Y) = \alpha_6 - \alpha_5 Y , \qquad (30)$$

$$f_R(Y) = \frac{\alpha_2^2}{2\alpha_4} Y^2 - \left(\alpha_1 + \frac{\alpha_2}{2\alpha_4}(\alpha_3 - \alpha_5)\right) Y$$

$$- \frac{\alpha_2}{2\alpha_4} Y\sqrt{\alpha_2^2 Y^2 + 2[2\alpha_1\alpha_4 - \alpha_2(\alpha_3 - \alpha_5)]Y + (\alpha_3 - \alpha_5)^2}$$

Both function $f_T(Y)$ and $-f_R(Y)$ are shown in fig. 6. The steady states determined by $\dot{Y} = 0$ are represented by the intersections of the curves $f_T(Y)$ and $-f_R(Y)$. Of course the results agree with table 2. In analogy to electrical systems the function $f_T(Y)$ can be referred to as "chemical load line". On the other hand the function $f_R(Y)$ represents the characteristic of the reaction system.

By plotting $\dot{Y} = f(Y) = f_T(Y) - (-f_R(Y))$ one gets the dynamical diagram from which the character of the steady states can easily be recognised (fig. 7).

Stability is given in the case of $d\dot{Y}/dY < 0$, whereas $d\dot{Y}/dY > 0$ means instability. Of special interest is the case $d\dot{Y}/dY = 0$, $d^2\dot{Y}/dY^2 \neq 0$. Realizing this situation by suitably increasing (or decreasing) α_6 a small perturbation will initiate a transition to the other stable steady state [2].

5. Discussion

In this paper we have demonstrated how to modify the original FKN mechanism for the oscillating Belousov–Zhabotinskii reaction to obtain bistability. The mathematical model shows that under appropriate conditions hyperbola-like curves (isoclines) generally associated with chemical reactions can intersect three times thus establishing three steady states. Further-

more, applying quasistationarity technique for reducing the number of differential equations gives rise to the appearance of a nonmonotonic function (28) rather different from the usual cubic power series as for the van der Pol oscillator. The mathematical model agrees quite well with the experimental results. This statement is confirmed by a comparison of the temporal course of the concentration of bromide into the stable steady states after having applied both sub- and superthreshold stimuli and the calculation according to eq. (19). Moreover, the upper steady state concentration of bromide calculated from the model is in good accordance with the value observed experimentally. However, the model predicts a lower stable steady state at about 10^{-12} M and an unstable one at about 10^{-8} M concentration of bromide. Such low concentrations cannot be measured reliably by bromide sensitive electrodes [12,22]. So it is an open question whether or not there exist concentrations of bromide as low as predicted. If there are no experimental methods to answer this question it might be of academic interest only.

A somewhat more delicate problem arises from the assumption of reaction step (4) to be rate-determining. Certainly this is true if there is a sufficient amount of cerium(III). Otherwise the radical $BrO_2^{\bullet}$ will not be further converted to $HBrO_2$. By this the autocatalysis [(4) + 2(5)] will be blocked.

The necessity for improving the model can be seen by inserting the steady state value $X_{ss}^{(3)}(HBrO_2)$ into eq. (10) and taking $\dot{Z} = 0$. Depending on Z_0 it is possible to obtain even negative concentrations of cerium(III). From this we conclude that cerium(III) in this case has dropped to such a low value that reaction step (5) must be taken into account. On the other hand we tried various concentrations of cerium(III) and found more or less the same overall behavior as illustrated in fig. 2. That is why we regard our model to be suitable for describing the multiple steady state situation experimentally observed in the CSTR.

Acknowledgement

The authors are grateful to Professor Dr. U. Franck for his interest in this work and for his support.

This research was supported in part by the Deutsche Forschungsgemeinschaft (Sonderforschungsbereich 160).

References

[1] P. Glansdorff and I. Prigogine, Thermodynamic Theory of Structure, Stability and Fluctuations (Interscience, Wiley, New York, 1971).
[2] U.F. Franck, in: Biological and Chemical Oscillators (Academic Press, New York, 1973).
[3] T. Matsuura and M. Kato, Chem. Eng. Sci. 22 (1967) 171.
[4] E. Wicke, Chem. Ing. Technik 46 (1974) 365.
[5] A.A. Andronov and C.E. Chaikin, Theory of Oscillations (Princeton University Press, Princeton, 1949).
[6] U.F. Franck, Studium Generale 18 (1965) 313.
[7] H. Degn, Nature 217 (1968) 1047.
[8] G. Waßmuth, Thesis, RWTH Aachen, Germany (1970).
[9] W. Geiseler, Thesis, RWTH Aachen, Germany (1974).
[10] A. Winfree, B.L. Clarke and R.M. Noyes, in: Faraday Symposia of the Chemical Society No. 9, Physical Chemistry of Oscillatory Phenomena, General Discussion (1974).
[11] R.M. Noyes, R.J. Field and R.C. Thompson, J. Am. Chem. Soc. 93 (1971) 7315.
[12] R.J. Field, E. Körös and R.M. Noyes, J. Am. Chem. Soc. 94 (1972) 1494.
[13] R.J. Field and R.M. Noyes, J. Chem. Phys. 60 (1974) 1877.
[14] A.M. Zhabotinskii, Kinetika i Kataliz 10 (1969) 83.
[15] N. Minorsky, Nonlinear Oscillations (Van Norstrand, Princeton, N.J., 1962).
[16] C.W. Gear, Numerical Initial Value Problems in Ordinary Differential Equations (Prentice–Hall, Englewood Cliffs, N.J., 1971).
[17] J.O. Hirschfelder, J. Chem. Phys. 26 (1957) 271.
[18] D. Edelson, J. Comput. Phys. 11 (1973) 455.
[19] R.J. Gelinas, J. Comput. Phys. 9 (1972) 222.
[20] A.C. Hindmarsh, Lawrence Livermore Laboratory, Livermore, California 94 550.
[21] K.F. Bonhoeffer, Naturwiss. 40 (1953) 301.
[22] J.H. Woodson and H.A. Liebhafsky, Anal. Chem. 41 (1969) 1894.
[23] H.H. Föllner and W. Geiseler, in preparation.